PRELIMINARY EXPERIMENTAL RESULTS FOR INDIRECT VECTOR CONTROL OF INDUCTION MOTOR DRIVES WITH FORCED DYNAMICS

Ján VITTEK*, Ján MICHALÍK*, Stephen J. DODDS and Roy PERRYMAN****

**University of Žilina, Faculty of Electrical Engineering, Veľký diel ND, 010 26 Žilina, Slovak Republic, tel.: +421 41 513 2155, e-mail: vittek@fel.utc.sk, michalik@fel.utc.sk*

***University of East London, School of Computing Engineering, Longbridge Road, Dagemham, Essex, RM8 2AS, United Kingdom, tel.: +44 208 223 2379, e-mail: s.j.dodds@uel.ac.uk, r.perryman@uel.ac.uk*

Summary The contribution presents an extension of indirect vector control of electric drives employing induction motors to *'Forced Dynamic Control'*. This method of control offers an accurate realisation of dynamic response profiles, which can be selected by the user. The developed system can be integrated into a drive with a shaft position encoder or a shaft sensorless drive, in which only the stator currents are measured. The applied stator voltages are determined by a computed inverter switching algorithm. Simulation results and preliminary experimental results for indirect vector control of an idle running induction motor indicate good agreement with the theoretical predictions.

Keywords: Vector control of induction motor, Forced dynamic control, Shaft sensorless control

1. INTRODUCTION

The result of the proposed approach to the shaft sensorless indirect vector control of induction motors (IM) [1], [2] is a new control law, which may be operated in any one of the following modes, according to the application:

a) Direct acceleration control where the drive produces a rotor shaft angular acceleration following a demanded acceleration with negligible dynamic lag, with piecewise constant acceleration.
b) Direct acceleration control where the drive produces a rotor shaft angular acceleration following a demanded acceleration with negligible dynamic lag, with continuous linearly increasing and decreasing acceleration during speed-up.
c) Linear first order speed response, where the drive behaves as a first order linear system with a prescribed time constant, to facilitate the design of a linear control system employing the drive.
d) Linear second order speed response, where the drive acceleration is prescribed such that the closed-loop system has a response determined by a prescribed second order characteristic equation.

The structure of the drive control system based on indirect vector control is shown in Fig. 1. The outer control loop creates the torque and flux components of the demanded stator currents. While computation of the flux component completely corresponds to the standard indirect vector control method, the computation of the torque component is based on the developed algorithm, which realises the prescribed closed-loop dynamic behaviour of the selected operational mode, without any need for 'trial and error' based adjustments. For the shaft encoder version, the desired electrical angle, ρ_e, for the reference frame transformation, is obtained as a sum of the real rotor position, θ_r, and the integral of computed slip frequency, ω_{sl} *(dashed lines)*. To achieve the prescribed speed response with minimal influence of external disturbances, the master control law requires an estimate of the load torque gained in the observer model, which is based on the motor mechanical equation. The inner control loop then forces the three-phase stator currents to follow their computed demands with negligible dynamic lag by setting the switching state of the three-phase inverter to oppose the errors between the demanded and measured stator currents at the beginning of every iteration interval.

For shaft sensorless applications, the drive control system contains a set of three observers for estimation of the rotor magnetic flux, rotor speed and the load torque. Since the only measurement variables are the stator currents and the applied stator voltages being determined by the computed switching algorithm of inverter and with a knowledge of the dc link voltage the rotor flux observer is based on these inputs only. A rotor speed estimator which operates in a pseudo-sliding mode and requires just these aforementioned measurements together with estimated rotor flux components from a magnetic flux estimator, is employed for rotor speed estimation. A filtering observer whose real time model is again based on the motor mechanical equation produces filtered rotor speed and load torque estimates required by the outer loop control law. This observer requires the output of the pseudo-sliding mode speed estimator, the measured stator current components and estimated magnetic flux components as inputs. The rotor position estimate is gained by integration of the estimated rotor speed. When operating without the shaft sensor, the control system, as developed to date, would be suited very well to applications requiring control to a moderate accuracy.

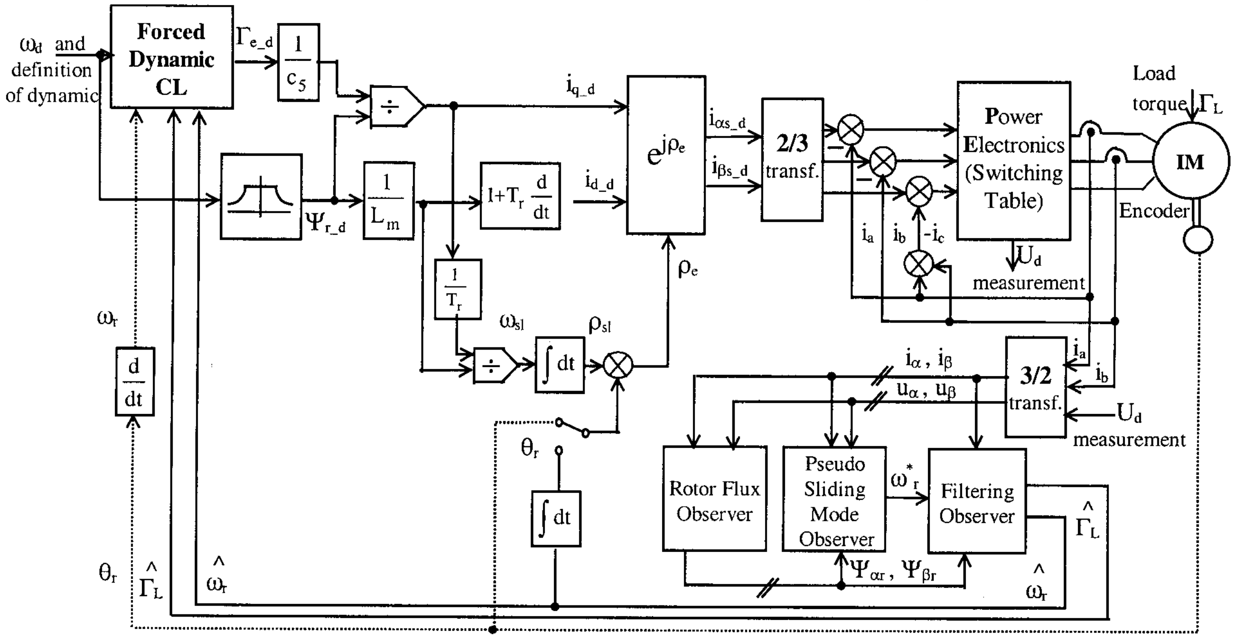

Fig. 1 Overall control system block diagram

2. THE CONTROL LAW DEVELOPMENT

The basic philosophy in the control law development is to satisfy the conditions for indirect vector control and to prescribe a profile of speed and acceleration during start-up [3], [4]. This is achieved through feedback linearisation principles [5], [6]. For the rotor speed response is formulated the linearising function, which forces the rotor speed to obey a specified closed-loop differential equation. Firstly mode (c) in section 1 is considered, in which this differential equation is assumed linear, first order with time constant, T_ω.

2.1. Model of Induction Motor

The IM model for stator currents and rotor fluxes is formulated in the (x_y) co-ordinate system, which rotates at the eligible rotational speed, ω_k :-

$$\dot{\mathbf{I}}=c_1\left[\mathbf{U}-a_1\mathbf{I}+c_2\mathbf{P}(\omega_r)\mathbf{\Psi}\right]-\omega_k\mathbf{T}^T\mathbf{I} \tag{1}$$

$$\dot{\mathbf{\Psi}}=c_4\mathbf{I}-\mathbf{P}(\omega_r)\mathbf{\Psi}+\omega_k\mathbf{T}^T\mathbf{\Psi} \tag{2}$$

$$\dot{\omega}_r=\frac{1}{J}\left[c_5\mathbf{\Psi}^T\mathbf{T}^T\mathbf{I}-\Gamma_L\right];\quad \dot{\Gamma}_L=0 \tag{3}$$

where:

$$\mathbf{P}(\omega_r)=\begin{bmatrix} c_3 & p\omega_r \\ -p\omega_r & c_3 \end{bmatrix} \quad \text{and} \quad \mathbf{T}=\begin{bmatrix} 0 & -1 \\ 1 & 0 \end{bmatrix}$$

and where $\mathbf{\Psi}^T=\left[\Psi_x \ \ \Psi_y\right]$ is the rotor magnetic flux, $\mathbf{I}^T=\left[i_x \ i_y\right]$ is the stator current, $\mathbf{U}^T=\left[u_x \ u_y\right]$ is the stator voltage, ω_r is the mechanical rotor speed, the individual constants are given by:- $c_1=L_r/\left(L_sL_r-L_m^2\right)$, $c_2=L_m/L_r$, $c_3=R_r/L_r=1/T_r$, $c_4=L_m/T_r$, $c_5={}^{3pL_m}\!/_{2L_r}$, $a_1=R_s+\left(L_m^2/L_r^2\right)R_r$

and where L_s , L_r and L_m are, respectively, the stator and rotor inductances and their mutual inductance. R_s and R_r are, respectively, the stator and rotor resistance and p is the number of stator pole pairs.

2.2. The Master Control Law Development

To achieve complete rotor flux field orientation for indirect vector control it is necessary to satisfy following conditions for both stator current components and for the slip rotor frequency [2], which are already included in the control system block diagram of Fig.1:

$$i_{q\_d}=\frac{T_{e\_d}}{c_5\Psi_{r\_d}} \tag{4}$$

$$i_{d\_d}=\frac{1}{L_m}\left(\Psi_{r\_d}+T_r\frac{d\Psi_{r\_d}}{dt}\right) \tag{5}$$

$$\omega_{sl}=\frac{1}{T_r}\left(\frac{L_m i_{q\_d}}{\Psi_{r\_d}}\right) \tag{6}$$

The control law, which realises various prescribed dynamics, is derived using the feedback linearisation principles [5], [6] for the field oriented rotating reference frame model of IM, where de-coupling between *d*- and *q*-axes is achieved. Firstly, a *linearising function* is formulated which forces the rotor speed to obey the following linear, first order closed-loop differential equation with specified time constant T_ω:

$$\dot{\omega}_r = \frac{1}{T_\omega}(\omega_d - \omega_r) = acc_d \quad (7)$$

The linearising function for $\dot{\omega}_r$ is then obtained simply by equating the right hand sides equations (3) and (7):-

$$\mathbf{\Psi}^T \mathbf{T}^T \mathbf{I} = \frac{1}{c_5}\left[\frac{J}{T_\omega}(\omega_d - \omega_r) + \Gamma_L\right] \quad (8)$$

In ideal field orientation the total rotor flux linkage is forced to be aligned with the d-axis. The flux linkage and its derivative in the q-axis are therefore set to zero. For constant rotor flux operation up to the nominal speed, the flux component i_d is kept constant and then the rotor flux is given by:

$$\mathbf{\Psi}_r = \Psi_D = L_m i_d \quad (9)$$

The required control law is then obtained by combining equations (7), (8) and (9), but before this is done, the state variables (x) are replaced by their estimates, $(\tilde{x})$ from the observers for the shaft sensorless version. Also, the constant motor parameters (p) are replaced by estimates $(\tilde{p})$ as these are the known parameters. Thus:

$$i_{d\_d} = const$$

$$i_{q\_d} = \frac{\frac{\tilde{J}}{T_\omega}(\omega_d - \tilde{\omega}_r) + \tilde{\Gamma}_L}{c_5 L_m i_{d\_d}} = \frac{\Gamma_{e\_d}}{c_5 \Psi_D^*} \quad (10)$$

where:

$$\Gamma_{e\_d} = \Gamma_{acc} + \tilde{\Gamma}_L = \tilde{J} \cdot acc_d + \tilde{\Gamma}_L \quad (11)$$

The derived control algorithm for the electrical torque of an IM consists of two parts. The first of them creates the inertial torque for the demanded output acceleration, acc_d , of the shaft and the second part counteracts the load torque. With this knowledge, the aforementioned operational modes can be realised by means of four different equations for acc_d. It should be noted that the external load torque, Γ_L, is treated as a state variable in the observer where it is estimated together with the other state variables. It is assumed constant in formulation of the state equations but the observer can follow time varying load torques with sufficient accuracy when the observer poles are given sufficiently high values.

2.2.1. The acceleration for piecewise constant torque [operational mode (a)]

In this case, demanded acceleration is determined by a constant demanded angular velocity, ω_d, and a demanded acceleration time, T_s.

$$acc_d = \frac{\omega_d}{T_s} \operatorname{sign}[\omega_d - \omega_r] \quad (12)$$

The electrical torque realising this is then determined by equation (11).

2.2.2. The acceleration for linearly increasing and decreasing torque [operational mode (b)]

For this operational mode, the acceleration during speed-up is linearly increasing up to half of the demanded speed and then is linearly decreases to zero. The value of the acceleration derivative, jerk, 'ε' during speed-up is constant and the maximum acceleration occurs in the middle of this interval. This demanded acceleration is realised by the following equations:

$$\varepsilon = \frac{4}{T_s^2}\omega_d \quad (13a) \qquad acc_{max} = \frac{2}{T_s}\omega_d \quad (13b)$$

$$acc_d = \varepsilon t \cdot \operatorname{sign}(\omega_d - \omega_r) \quad \text{for } t \in \left(0, \frac{T_s}{2}\right)$$
$$acc_d = \varepsilon T_s\left(1 - \frac{t}{T_s}\right) \cdot \operatorname{sign}(\omega_d - \omega_r) \text{for } t \in \left(\frac{T_s}{2}, T_s\right) \quad (14)$$

2.2.3. The acceleration for first order dynamics [operational mode (c)]

This case has already been covered during the master control law development (ref., equation (7):

$$acc_d = \frac{3}{T_s}(\omega_d - \omega_r) \quad (14)$$

2.2.4. The acceleration for second order dynamics [operational mode (d)]

In this case, the derivative of the demanded acceleration obeys (15a) and the desired closed-loop differential equation for the rotor acceleration is realised by (15c).

$$\ddot{\omega}_r = -2\xi\omega_{nat}\dot{\omega}_r + \omega_{nat}^2(\omega_{dem} - \omega_r) \quad (15a)$$

If critical damping is chosen then the damping ratio is $\xi = 1$ and the poles of the closed-loop system are coincident enabling the settling time formula (15b) (*where n is order of the system*) to be used to determine ω_n to realise a chosen settling time:

$$T_{settl} = 1.5 * (1+n)\frac{1}{\omega_{nat}} \quad (15b)$$

Equation (15a) is then numerically integrated with $\dot{\omega}_r$ replaced by the demanded angular acceleration, acc_d, and ω_r by its estimate, $\hat{\omega}_r$. Thus:-

$$acc_d := acc_d + \left[\omega_{nat}^2\left(\omega_{dem} - \hat{\omega}_r\right) - 2\xi\omega_{nat}acc_d\right] * h \qquad (15c)$$

The ideal acceleration and speed responses based on the four different prescribed dynamic modes are shown in Fig. 2.

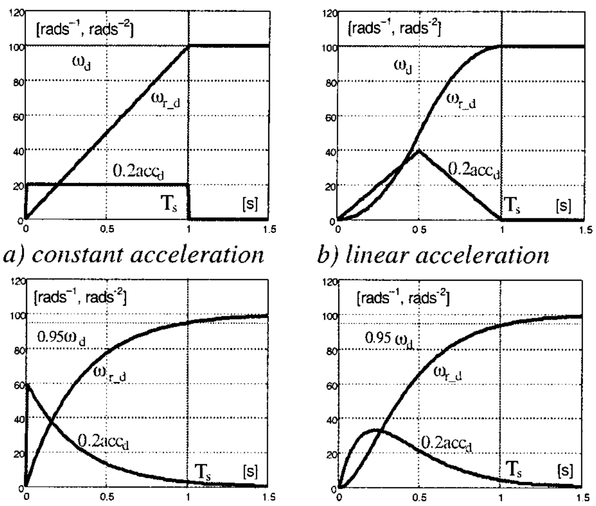

a) constant acceleration *b) linear acceleration*

c) first order dynamics *d) second order dynamics*

Fig. 2 Prescribed profiles of acceleration and speed for individual dynamic modes

2.3. Slave Control Law

The sub-plant to be controlled here is defined by equation (1), the control variable now being **U** and the output variable, **I**, to respond to the demanded current vector, $\mathbf{I_d}$. The slave control law is the following **bang-bang control law**:-

$$\mathbf{U} = U_{max}\,\mathbf{sgn}\left[\mathbf{I}_d - \mathbf{I}\right] \qquad (16)$$

This bang-bang control law is intended to operate in the sliding mode with a rapidly switching control variable. This ideally maintains $\mathbf{I}=\mathbf{I_d}$ with an infinite switching frequency of the control variables. In practice, a finite but high switching frequency (*7 kHz*), maintains a relatively low amplitude limit cycle.

3. ESTIMATION AND FILTERING

Even if rotor position or velocity feedback are available the derived master control law requires as an input the estimate of load torque a direct measurement of this being assumed unavailable. The load torque observer must be therefore be an integral part of the control system.

3.1. Version with Shaft Encoder

The real time model of the load torque observer is based on the differential equations for the motor position and its speed, together with a differential equation for the load torque. The load torque is treated as a state variable, but a precise differential equation cannot be written down for this, as its form is unknown, but good results are attainable by assuming that the load torque is constant. Hence, the real plant is described by the three state differential equations (17a). The observer equations (17b) comprise a real-time model based on (17a) together with additional error correction terms using the error between the measured and estimated rotor positions, i.e., $e_\Theta = \Theta_r - \hat{\Theta}_r$.

$$\begin{aligned} \dot{\Theta}_r &= \omega_r \\ \dot{\omega}_r &= \frac{1}{J}\left[c_5\mathbf{\Psi}^T\mathbf{T}^T\mathbf{I} - \Gamma_L\right] \qquad (17a) \\ \dot{\Gamma}_L &= 0 \end{aligned}$$

$$\begin{aligned} \dot{\hat{\Theta}}_r &= \hat{\omega}_r + k_\Theta e_\Theta \\ \dot{\hat{\omega}}_r &= \frac{1}{J}\left[c_5\mathbf{\Psi}^T\mathbf{T}^T\mathbf{I} - \hat{\Gamma}_L\right] + k_\omega e_\Theta \qquad (17b) \\ \dot{\hat{\Gamma}}_L &= 0 + k_\Gamma e_\Theta \end{aligned}$$

where $\hat{\Theta}_r$, $\hat{\omega}_r$ and $\hat{\Gamma}_L$ are, respectively estimates of Θ_r, ω_r and Γ_L. Thus the observer correction loop is actuated by the error between the measured rotor position and its estimate from the observer as can be seen from Fig. 3a. Equations (17b) are now numerically integrated by the Euler explicit formula using the iteration interval corresponding to the achieved sampling frequency.

Equations (17b) define a conventional third order linear observer with a correction loop characteristic polynomial, which may be chosen via the gains k_Θ, k_ω and k_Γ. If all three observer poles are placed at $s=-\omega_0$, then the filtering time constant, $T_f = 1/\omega_0$, is a single design parameter. By equating the observer characteristic polynomial with the prescribed one the gains can be calculated as follows:-

$$s^3 + \frac{18}{T_f}s^2 + \frac{108}{T_f^2}s + \frac{216}{T_f^3} = s^3 + k_\Theta s^2 + k_\omega s + \frac{k_\Gamma}{J} \qquad (18a)$$

$$k_\Gamma = \frac{216J}{T_f^3};\ k_\omega = \frac{108}{T_f^2};\ k_\Theta = \frac{18}{T_f};\ \text{for } T_f = \frac{6}{\omega_0} \qquad (18b)$$

The selection of ω_0 should be restricted by a rule of thumb which is $\omega_0 < 5/h_0$ to ensure that the discrete time correction loop behaviour approximates to that of the theoretical continuous observer, otherwise oscillations of the estimates at a frequency of $1/2h_0$ may occur, or even instability.

Although the load torque is assumed constant in the formulation of its real time model, the estimate, $\tilde{\Gamma}_L$, will follow an arbitrarily time varying disturbance torque and will do so more closely as T_f is reduced but at the expense of sensitivity to any noise in the rotor position measurement. For a speed controlled drive in which only the rotor speed is measured, then the alternative second order observer of Fig. 3b can be employed with recalculated gains.

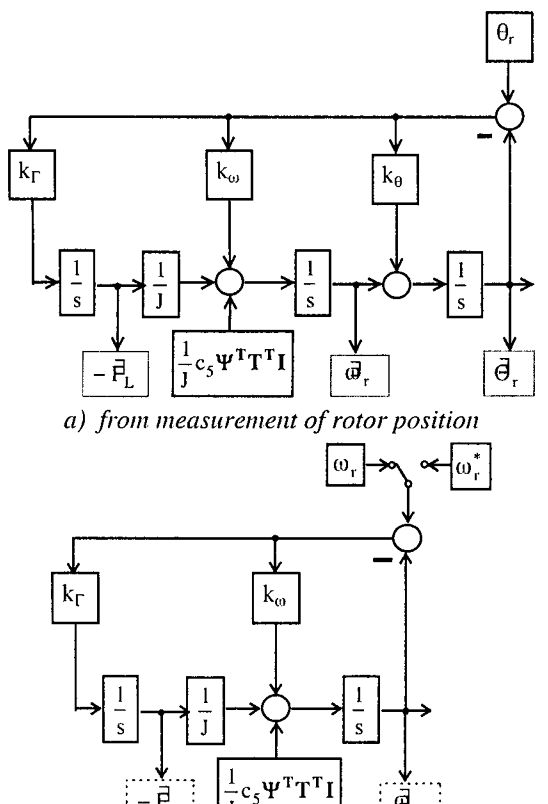

a) from measurement of rotor position

b) from measurement of rotor speed

Fig. 3 Filtering observer for estimation of the load torque and filtering rotor speed estimate

3.2. Shaft Sensorless Version

For this version the rotor magnetic flux, rotor speed and load torque estimates, which are inputs required by the master control law, are produced in a set of three observers [3], [4]. These are formulated in the (α_β) frame coupled to the stator of the IM. The observer system as developed to date is suitable for reliable operation in the speed range of $0.05\omega_{nom}$ up to $2\omega_{nom}$. The following description of these observers is therefore only brief.

3.2.1. The rotor magnetic flux estimator estimates the rotor flux vector components without requiring a knowledge of the rotor speed and is derived simply by eliminating the term, $\mathbf{P}(\omega_r)\Psi$, between equations (1) and (2):-

$$\Psi = \int\left[\left(c_4 - \frac{a_1}{c_2}\right)\mathbf{I} + \left(\frac{1}{c_2}\right)\mathbf{U}\right]dt - \left(\frac{1}{c_1 c_2}\right)\mathbf{I} \tag{19}$$

This was implemented using simple explicit Euler numerical integration. The integration, however, would be subject to long-term drift in practice and special measures should be taken to correct for this. More sophisticated flux observers described in [7] and [8] are strong candidates for further consideration.

3.2.2. The pseudo sliding mode observer is used to determine a primary, unfiltered estimate of the rotor speed. Firstly a stator current vector *pseudo sliding-mode* observer is formulated for generation of an unfiltered estimate, $\tilde{c}_1\tilde{c}_2\mathbf{P}(\omega_r^*)\Psi^*$ of the term, $c_1 c_2 \mathbf{P}(\omega_r)\Psi$, of equation (1), by means of the *equivalent control method* [9], from which is extracted an unfiltered estimate, ω_r^* of ω_r, with the aid of the flux estimate, Ψ^*, from the rotor flux estimator. The real-time model and correction input of this stator current vector based observer is given by:

$$\dot{\mathbf{I}}^* = \tilde{c}_1\left[-\tilde{a}_1\mathbf{I}^* + \mathbf{U}\right] - \mathbf{v} \tag{20}$$

where, $\mathbf{I}^*$ is an estimate of $\mathbf{I}$ as in a conventional observer. The required estimate, however, is not $\mathbf{I}^*$ but the continuous value of the correction input vector, $\mathbf{v}$, which completes the correction loop of the *pseudo-sliding-mode* observer according to:-

$$\mathbf{v} = -\mathbf{K}_I\left[\mathbf{I} - \mathbf{I}^*\right] \tag{21}$$

where $\mathbf{K}_I$ is diagonal matrix with relatively high gain elements, k_i, so that vector $\mathbf{v}$ is continuous. Then assuming that $\mathbf{I}^* = \mathbf{I}$, and replacing Ψ and ω_r, respectively, by their estimates, Ψ^* and ω_r^*, it is possible to derive:-

$$\mathbf{v}_{eq}^* = -\tilde{c}_1\tilde{c}_2\mathbf{P}(\omega_r^*)\mathbf{\Psi}^* \tag{22}$$

The unfiltered speed estimate, ω_r^*, is extracted by subtracting the two components of equation (22) yielding:-

$$\omega_r^* = \left[\mathbf{v}_{eq}^*\right]^T \mathbf{T}\mathbf{\Psi}^* \Big/ \left(\tilde{c}_1\tilde{c}_2 p \|\mathbf{\Psi}^*\|\right) \tag{23}$$

Control chattering is eliminated from this observer by replacement of relay switching functions of the basic sliding mode observer with the high gain equation (21). Another possibility for elimination of such chattering is described in [10].

3.2.3. The filtering observer produces a filtered angular velocity estimate, $\hat{\omega}_r$ together with external load torque estimate $\hat{\Gamma}_L$. The external load torque, Γ_L, is again treated as a state variable, which is constant. As previously, the real time model of this observer is based on the motor torque equation and therefore the continuous time version of observer is as follows:

$$\begin{aligned} e_\omega &= \omega_r^* - \hat{\omega}_r \\ \dot{\hat{\omega}}_r &= \frac{1}{\tilde{J}}\left[\tilde{c}_5 \mathbf{\Psi}^T\mathbf{T}^T\mathbf{I} - \hat{\Gamma}_L\right] + k_\omega e_\omega \\ \dot{\hat{\Gamma}}_L &= k_\Gamma e_\omega \end{aligned} \tag{24}$$

This is again a conventional second order linear observer with a correction loop characteristic polynomial, which may be chosen via the gains, k_ω and k_Γ, to yield a desired balance of filtering between the noise from the measurements of the currents i_α and i_β and the noise from velocity estimate) ω_r^* *(treated as a measurement)*. If the observer poles are placed at two different locations, $-\omega_1$ and $-\omega_2$, the observer gains k_ω and k_Γ can again be determined by equating the observer characteristic polynomial to the prescribed one. Thus:

$$s^2 + s(\omega_1 + \omega_2) + \omega_1\omega_2 = s^2 + s\cdot k_\omega + \frac{k_\Gamma}{J} \tag{25a}$$

$$k_\omega = (\omega_1 + \omega_2) \quad \text{and} \quad k_\Gamma = J\cdot\omega_1\cdot\omega_2 \tag{25b}$$

The block diagram of this version of filtering observer is shown in Fig. 3(b).

4. SIMULATION AND EXPERIMENTAL RESULTS

The parameters of the IM and ancillary devices used for simulation and preliminary experimental results are listed in the Appendix. Firstly, the shaft sensorless version of indirect vector control with forced dynamics was investigated by simulation, operated in all the four prescribed dynamic modes for the same speed demand of ω_{dem}=100 rad/s and settling time T_s=0.15 s. The dc bus voltage was assumed as U_{dc}=240 V, and therefore the load torque was 1 Nm (*1/4 of nominal*), applied at t=0.2s. The magnetic flux creating component of the current demand was kept constant at i_{d_d}=0.9 A to keep rotor flux approximately at Ψ_d=0.45 Wb.

In all the graphs presented, the stator currents are displayed as functions of time during the time interval t∈(0 - 0.25) s in subplots (a). The corresponding estimates of the rotor flux components for the same time interval are shown in subplots (b). Subplots (c) show the electrical torque of the motor, the external load torque and its estimate from filtering observer. Finally, subplots (d) show the ideal speed response together with the computed real rotor speed and its estimate from the filtering observer for the same time interval.

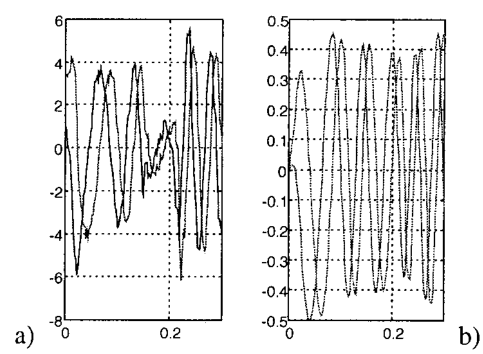

a) stator currents and b) rotor fluxes

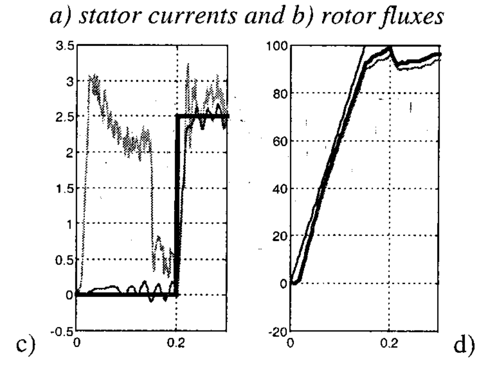

c) applied and estimated load torque, electrical torque

d) ideal, estimated and real rotor speed

Fig. 4a. Simulation results for constant acceleration

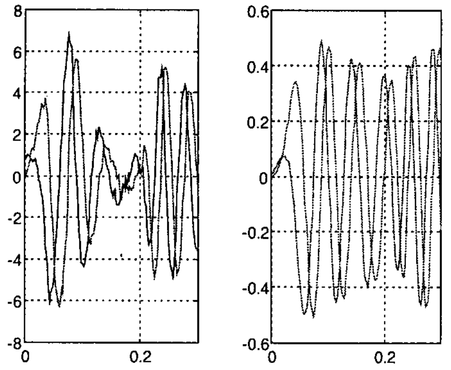

a) stator currents and b) rotor fluxes

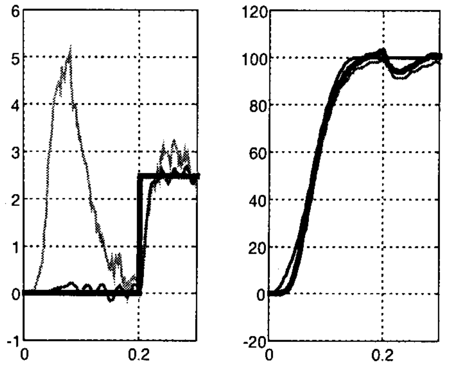

c) applied and estimated load torque, electrical torque
d) ideal, estimated and real rotor speed

Fig. 4b. Simulation results for linear acceleration

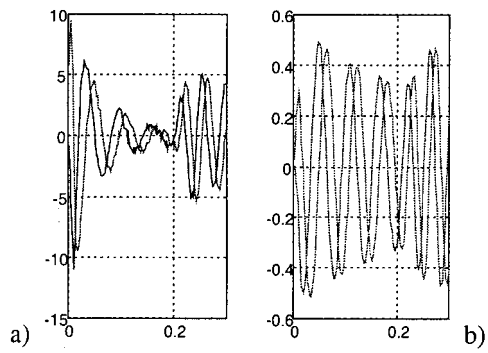

a) stator currents and b) rotor fluxes

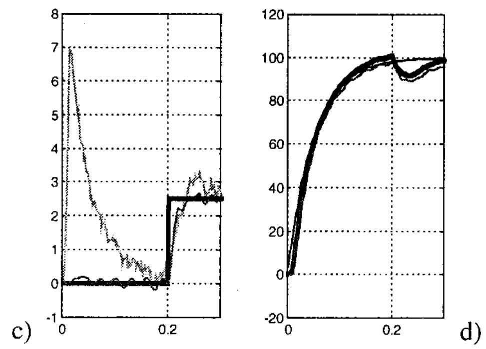

c) applied and estimated load torque, electrical torque
d) ideal, estimated and real rotor speed

Fig. 4c. Simulation results for first order dynamics

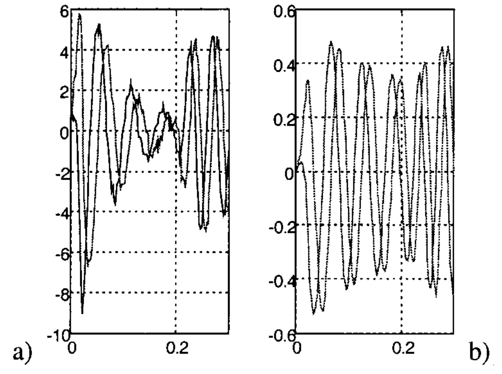

a) stator currents and b) rotor fluxes

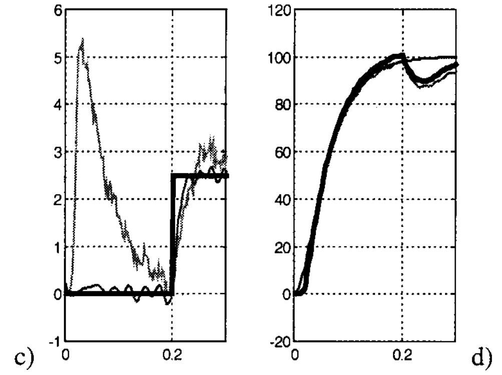

c) applied and estimated load torque, electrical torque
d) ideal, estimated and real rotor speed

Fig. 4d. Simulation results for second order dynamics

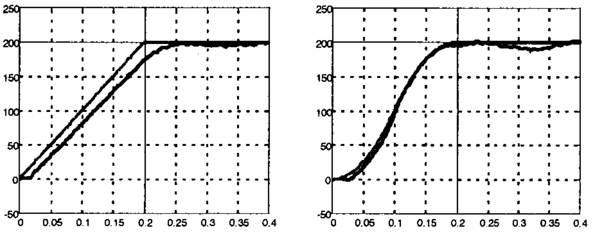

a) constant acceleration *b) linear acceleration*

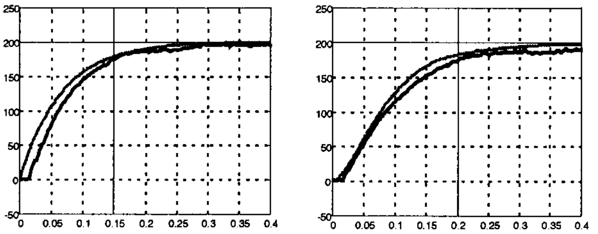

c) first order dynamic *d) second order dynamic*

Fig. 5. Experimental results for shaft direct vector control of IM with prescribed dynamics

It can be clearly observed in Fig. 4a to Fig. 4d, by comparison of the simulated rotor speed with the computed ideal speed response, that the demanded dynamics were achieved with a very short delay.

Preliminary experimental results for indirect vector control of IM without load and all four prescribed dynamic modes are shown in Fig. 5. The vector control law was implemented via a Pentium PC166, the stator currents being measured through LEM transformers and evaluated using a PC Lab Card PCL818 built direct into the PC. An IGBT transistor module (SEMIKRON SKiiP 32 NAB12T1) was used as a three-phase inverter, with a dc bus voltage was equal U_{dc}=240 V. The IM was idle running during experiments.

5. CONCLUSIONS AND RECOMMENDATIONS

The investigations by simulation of the proposed indirect vector control method of induction motor with forced dynamics show a good agreement with the theoretical predictions. The significant, though not very large, departure from the ideal performance is due mainly to the non-zero iteration interval, h, and dynamic lag in the load torque estimation as well as due to errors in the motor and load parameter estimation. Due to the known prescribed dynamics, the control system can be further extended and improved with model reference adaptive control.

While the piecewise constant acceleration mode is suitable for the majority of industrial applications, the dynamic modes with linearly increasing and decreasing acceleration and prescribed linear second order transfer function can be very attractive for designers of cranes and elevators. Also some traction applications can benefit from such smoothly controlled acceleration. The control system, as developed to date, would be suitable for applications requiring sensorless speed vector control of induction motors to a moderate accuracy ($\approx 5\%$).

APPENDIX

IM parameters:

Rated power	P_n=1.1 kW,
Rated speed	n_n =2840 rpm,
Rated current	I_n =2.6/4.5 A, Y/D
Terminal voltage U=380/220 V, Y/D	

Parameters for equivalent circuit:

Stator inductance:	L_S=0.553 H
Rotor inductance :	L_R=0.553 H
Mutual inductance	L_m=0.536 H
Stator resistance	R_S=6.678 Ω
Rotor resistance	R_R=5.020 Ω
Moment of inertia	J=0.0023 kgm^2
Current sensors LEM	LTA 50P/SPI.

Acknowledgements: The authors wish to thank to Martin Hraško and Daniel Vanko for producing the preliminary experimental results and to the 'Czech and Slovak Joined Commission' together with the 'Slovak Grant Agency' VEGA for funding the research projects No.016/023, 'Analysis of the Modern Electric Drives' and research project No.106/603 in the frame of which this contribution was created.

REFERENCES

[1] Boldea, I., Nasar, S.A.: *Vector Control of AC Drives.* **CRC Press**, London 1992.

[2] Leonhard, W.: *Control of Electric Drives*, **Springer Verlag**, Berlin 1985.

[3] Dodds, S.J., Utkin, V.A., Vittek, J.: *Sensorless Induction Motor Drive with Independent Speed and Rotor Magnetic Flux Control - Part 1-Theoretical Background and Part 2-Simulation and Real Time Implementation.* **Journal of Electrical Engineering**, Vol.49, y.1998, No.7-9 and No. 9-10, pp.186-193 and pp.232-239.

[4] Dodds, S. J., Vittek, J., Mienkina, M.: *Implementation of a Sensorless Induction Motor Drive Control System with Prescribed Closed-Loop Rotor Magnetic Flux and Speed Dynamics.* **EPE'97** conference Proceedings, *Trondhaim, Norway*, Sept. 1997, Vol.4., pp. 4.492-4.497.

[5] Isidori, A.: *Nonlinear Control Systems.* 2nd edition, **Springer-Verlag**, Berlin, 1990.

[6] Kanellakopoulos, I.,Krein, P.T., Disilvestro, S.: *A New Controller-Observer Design for Induction Motor Control.* ***ASME,*** DSC-Vol.43, y.1992, 'Advances in Robust and Non/linear Control Systems', pp.43-47.

[7] Roboam, X., Andrieux, C., de Fornel, B., Hapiot, J.C.: *Rotor Flux Observation and Control in Squirrel Cage Induction Motor: Reliability with Respect to Parameters Variations.* **IEE Proceedings-D**, Vol. 139, No.4, July 1992, pp.363-370.

[8] Turl, G., Summer, M., Asher, G.M.: *A High Performance Sensorless induction Motor Drive for use in Multi-Motor Speed Synchronised Applications.* **EPE-2001** conference, *Graz, Austria*, Sept.2001, CD-Rom.

[9] Utkin, V.I. *Sliding Modes in Control and Optimisation*, **Springer.Verlag**, Berlin 1992.

[10] Nagy, L., Petersztegi, S., Mezo, T., Knerczer, G., Korondi, P.: *Brushless Motor Drives in Vehicle Applications.* **Journal of Electrical Engineering,** Polytechnica Publishing House, Romania, vol.2, 2002. http://www.jee.ro.

[11] Orlowska-Kowalska, T., Wojsznis, P., Kowalski, C.T.: *Dynamical Performances of Sensorless*

Induction Motor Drives with Different Flux and Speed Observers. **EPE-2001** conference, *Graz, Austria*, Sept.2001, CD-Rom.

[12] Korondi, P., Young, D.K., Hashimoto, H.: *Sliding Mode Based Disturbance Compensation for Motion Control.* **IEEE IECON'97** conference Proceedings, New Orleans, Louisiana, Nov.1997, pp.73-78.

[13] Law, C.M., Lin, F.J., Kung, Y.S.: *Design and Implementation of a High Performance Induction Motor Servodrive.* **IEE Proceedings-B**, Vol.140, No.4, july 1993, pp.241-246.

[14] Dobrucký, B., Špánik, P.: .: *Modelovanie a simulácia výkonových polovodičových štruktúr.* **EDIS** Žilina 1999

[15] Brandštetter, P., Vinklárek, D., Palacký P.: *A Comparison of Estimation Techniques for Realisation of Sensorless Induction Motor Drives.* **EDPE'01** conference proceedings, Podbanské, Slovakia, Oct. 2001, pp.214-218.

[16] Fedor, P., Perduková, D., Timko, J.: *Study of Controlled Structure Properties with Reference Model.* **Acta Technica** CSAV *Prague, Czech Republic*, No.46, pp.167-179.

[17] Urbanski, K., Zawirski, K.: *Sensorless Control of PMSM with Modiefied Observer Structure.* **EPE-PEMC'02** conference, *Cavtat, Croatia*, Sept. 2002, CD-Rom.

[18] Krzeminski, Z., Jaderko, A.: *A Speed Observer System of Induction Motor with Magnetizing Curve Identification.* Proceedings of **EPE - PEMC'00** conference, Kosice, Slovak Republic, Sept.2000, Vol.6, pp. 6-109 - 6-113.

[19] Wlas, M., Krzeminski, Z.: *Neural Network Based Tuning of Speed Observer for Control of Induction Motor.* **EPE-PEMC'02** conference, Cavtat, Croatia, Sept. 2002, CD-Rom.

[20] Žilková, J., Timko, J., Fedák, V.: *Estimation of Induction Motor Variables based on ANN Utilizing Apriori Information.* **EPE-2001** conference, Graz, Austria, Sept.2001, CD-Rom.

[21] Zboray, L., Ďurovský, F.: *Regulované pohony.* **Vienala** Kosice 2000.

[22] Fedor, P., Fedák, V., Bober, P., Timko, J.: *Field Oriented Induction Motor Drive with Indirect Rotor Flux Sensing.* 4th **EPE'91** conference, Florence 1991, pp. 214 -. 217.

[23] Ohtani, T., Takada, N., Tanaka, K.: *Vector Control of Induction Motor without Shaft Encoder.* **IEEE Transactions** on Industry Applicatios, 1992, Vol.28, No.1, pp.157-164.

Abstrakt: Príspevok sa zaoberá rozšírením nepriameho vektorového riadenia elektrických pohonov s asynchrónnymi motormi o '*riadenie s vnútenou dynamikou*'. Táto riadiaca metóda ponúka presnú realizáciu priebehov dynamických oziev, ktoré si môže vybrať užívateľ. Vyvinutý riadiaci systém môže byť integrovaný do pohonu so snímačom polohy na hriadeli alebo bez snímača, kedy sa merajú iba prúdy statora. Priložené napätia statora sa určia zo spínacieho algoritmu striedača. Simulačné výsledky a predbežné experimentálne výsledky pre nepriame vektorové riadenie asynchrónneho motora v stave naprázdno vykazujú dobrú zhodu s teoretickými predpokladmi.